HHS Public Access

Author manuscript

Psychiatry Res. Author manuscript; available in PMC 2018 July 30.

Published in final edited form as:

Psychiatry Res. 2017 July 30; 265: 35–44. doi:10.1016/j.pscychresns.2017.05.005.

Aberrant Functional Connectivity in Incarcerated Male Adolescents with Psychopathic Traits

Sandra Thijssen[a,b] and **Kent A. Kiehl**[c,d,e]

[a]School of Pedagogical and Educational Sciences, Erasmus University of Rotterdam, the Netherlands [b]Center for Child and Family Studies, Leiden University, the Netherlands [c]The Mind Research Network, Albuquerque, NM, USA [d]Department of Neurosciences, School of Medicine, University of New Mexico, Albuquerque, NM, USA [e]Departments of Psychology, Neuroscience, and Law, University Of New Mexico, Albuquerque, New Mexico

Abstract

The present study examined the association between psychopathic traits and functional connectivity in 177 incarcerated male adolescents. We hypothesized that psychopathic symptoms would be associated with aberrant functional connectivity within networks encompassing limbic and paralimbic regions, such as the default mode (DMN), salience networks (SN), and executive control network (ECN). The present sample was drawn from the NIMH-funded Southwest Advanced Neuroimaging Cohort, Youth sample (SWANC-Y), and from research at a youth detention facility in Wisconsin. All participants were scanned at maximum-security facilities. Psychopathic traits were assessed using Hare's Psychopathy Checklist-Youth Version (PCL-YV). Resting-state networks were computed using group Independent Component Analysis. Associations between psychopathic traits and resting-state connectivity were assessed using Mancova analyses. PCL-YV Total score and PCL-YV Factor 1 score (interpersonal and affective traits) were associated with the power spectra of the DMN. PCL-YV Factor 1 score was associated with spatial map of the SN and the ECN. PCL-YV Factor 2 score (lifestyle and antisocial traits) was associated with spatial map of the ECN. Comparable to adult psychopathy, adolescent psychopathic traits were associated with networks implicated in self-referential thought, moral behavior, cognition, and saliency detection: functions which have previously have been reported to be disrupted in adult psychopaths.

Keywords

psychopathy; resting state fMRI; default mode network; salience network; juvenile delinquents; adolescence

Kent A. Kiehl, The Mind Research Network, 1101 Yale Blvd. NE, Albuquerque, New Mexico 87106, kkiehl@mrn.org; phone: +1 505-272-5028.

1. Introduction

Psychopathy is a serious mental health disorder characterized by interpersonal, affective and behavioral traits such as lack of guilt and remorse, glibness, and impulsivity (Hare, 2003). As psychopaths are prone to violence and very likely to re-offend after release from prison, psychopathy poses a severe societal problem (Hemphill et al., 1998). Research suggests that psychopathy is developmental in nature, with psychopathic traits becoming apparent before the age of 10 years (Viding et al., 2005). While popular dogma holds that adult psychopaths are relatively resistant to treatment (Kiehl and Hoffman, 2011), youth with elevated psychopathic traits may be susceptible to intervention programs (Caldwell et al., 2007). Moreover, compared to adults, the neural correlates of psychopathic traits in children and adolescents will be less affected by the behavior itself (reversed causality) and/or environmental influences (e.g. lead exposure) and are thus more likely to reflect etiology. Examining the neurobiology of psychopathic traits in adolescents may therefore provide important insights on the development of psychopathy as well as information relevant for treatment and prevention programs. Here, we examined the association between psychopathic traits and functional connectivity in a large sample of incarcerated male adolescents.

As implied by the wide range of emotional and behavioral symptoms that characterize the disorder, psychopathic symptoms in both adults and adolescents have been related to functional and structural differences in limbic and paralimbic structures, such as amygdala, hippocampus, parahippocampal regions, anterior and posterior cingulate cortex, insula, temporal pole and orbitofrontal cortex (OFC) (Cope et al., 2014; De Brito et al., 2009; Ermer et al., 2013; Harenski et al., 2014; Kiehl et al., 2001; Wallace et al., 2014; Yang et al., 2011). For example, psychopaths are reported to have decreased amygdala, hippocampal, OFC and temporal pole volume or thickness (Cope et al., 2014; Gregory et al., 2012; Yang et al., 2005). Moreover, psychopathy has been associated with aberrant activation in the amygdala, prefrontal and temporal cortex during moral decision-making (Harenski et al., 2010; Marsh and Cardinale, 2014) and while viewing emotional faces (Contreras-Rodriguez et al., 2014; Decety et al., 2014).

In recent years, there has been a significant increase in studies examining resting state functional connectivity. Functional connectivity, defined as the relation between the neuronal activation patterns of anatomically separated brain regions (Aertsen et al., 1989), describes the organization, inter-relationship and integrated performance of functionally coupled brain regions (Rogers et al., 2008). Thus, while task based fMRI studies provide information on brain functioning during specific behavior, resting state functional connectivity provides information on brain organization. Differences in functional connectivity have been related to several psychological disorders, such as autism and schizophrenia (e.g. Cerliani et al., 2015; Rashid et al., 2014). In adults, psychopathy has most markedly been associated with aberrant functional connectivity in (regions of) the default mode network (DMN), which includes the medial prefrontal cortex, posterior cingulate cortex, precuneus and angular gyrus (Juarez, et al., 2013; Motzkin et al., 2011; Pujol et al., 2012; Sheng et al., 2010). The default mode network has been implicated in self-processing and moral behavior (Andrews-Hanna, 2012; Buckner et al., 2008; Li et al.,), and aberrant functioning of this network may

play an important role in explaining core psychopathy symptoms, such as inflated sense of self (Hare, 2003), impaired emotion recognition (social perspective taking) (Dawel et al., 2012), and impaired moral decision making (Tassy et al., 2013). As the brain undergoes significant changes during adolescence and early adulthood (Gogtay et al., 2004), adult findings cannot simply be extrapolated to youth with elevated psychopathic traits. Nevertheless, several studies in adolescent samples have also reported associations between psychopathic traits and DMN connectivity (Aghajani et al., 2016; Cohn et al., 2015; Shannon et al., 2011). However, results by Broulidakis et al. (2016) suggest that the DMN is associated with conduct disorder, but not psychopathic traits. Besides the DMN, several other brain networks, such as the salience network (SN, insula, anterior cingulate cortex (ACC, amygdala) and executive control network (ECN, OFC), encompass paralimbic regions and may thus be involved in psychopathic behavior (Aghajani et al., 2016; Kiehl, 2006).

The present study examined the association between functional connectivity and psychopathic traits in a large sample of incarcerated adolescent boys. Based on prior resting state, but also task-based functional MRI and structural neuroimaging studies suggesting (para)limbic involvement in psychopathy (for example, Cope et al., 2014; De Brito et al., 2009; Ermer et al., 2013; Harenski et al., 2014; Kiehl et al., 2001; Pujol et al., 2012; Wallace et al., 2014; Yang et al., 2011), we hypothesized that psychopathic symptoms in incarcerated adolescents would be associated with functional connectivity within networks encompassing limbic and paralimbic brain regions, such as the DMN, SN, and ECN.

2. Methods

2.1 Participants

The present sample was drawn from the NIMH-funded Southwest Advanced Neuroimaging Cohort, Youth sample (SWANC-Y), collected between June, 2007, and May 2011 in a maximum-security facility in New Mexico and from ongoing (2011–15) research at a youth detention facility in Wisconsin. This research was approved by the University of New Mexico Human Research Review Committee. Youth provided written informed assent as well as parent/guardian written informed consent. Participants were excluded if they had a history of seizures, traumatic brain injury, psychosis, other major medical problems, or were not fluent in English at or above a grade four reading level. Resting state scans, and Psychopathy Checklist –Youth Version (PCL-YV) scores were available from n= 227 male adolescents. After excluding n= 9 for excessive motion or radiological findings and n= 17 who were met the above exclusion criteria after scanning, our final sample consisted of n= 201 participants. The sample contained 177 complete cases. Participants were paid a flat rate, yoked to the standard institutional hourly pay scale, for participation in the study.

2.2 Measures

2.2.1 Psychopathic Traits—Assessment with the PCL-YV includes a review of institutional records and a semi-structured interview regarding individuals' school, family, work, and criminal histories, and their interpersonal and emotional skills (Forth et al., 2003). Individuals are scored on 20 items that measure personality traits and behaviors

characteristic of psychopathy. Scores range from 0 to 40. For adults, the accepted diagnostic cutoff for psychopathy is 30 and above. However, due to developmental issues, this cutoff is not used for adolescents. Although technically there is no Factor 1 and 2 in the PCL-YV, for comparison to adult samples, we examined a two-factor model of psychopathic traits in addition to a Total PCL-YV score, with Factor 1 composed of interpersonal and affective traits and Factor 2 composed of lifestyle and antisocial traits. Factor 1 and 2 in youth were computed the same way it is done in adults (Hare, 2003).

This sample covered a wide range of PCL-YV scores, including a sufficient number of high scorers (PCL-YV >= 30, n = 56) indicating a high level of psychopathic traits. Interviews were conducted by trained researchers and videotaped for reliability assessment (12% of interviews (randomly selected) were double-rated; intra-class correlation coefficient (ICC 1,1) = 0.90 for PCL-YV Total score).

2.2.2 IQ—IQ was estimated from the Vocabulary and Matrix Reasoning sub-tests of the Wechsler Adult Intelligence Scale-Third Edition for participants older than 16 years of age, and from the Wechsler Intelligence Scale for Children–Fourth Edition for participants younger than 16 years of age (Wechsler, 1997, 2003).

2.2.3 Substance use—Trained researchers administered the Kiddie Schedule for Affective Disorders and Schizophrenia (KSADS) (Kaufman et al., 1997). From the KSADS, we examined what substances were used. Moreover, for alcohol and cannabis, participants were asked how many months they used regularly (3 or more times/week). To approach a normal distribution, the duration of alcohol abuse was log transformed. During MRI assessment, all participants were in forced abstinence, many for at least 6 months.

2.2.4 Attention deficit hyperactivity disorder—Attention deficit hyperactivity disorder (ADHD) was diagnosed by trained researchers using KSADS.

2.2.5 Imaging data—All participants were scanned at the maximum-security facilities using The Mind Research Network's 1.5 T Avanto SQ Mobile MRI scanner. We used an EPI gradient-echo pulse sequence with TR/TE 2000/39 ms, flip angle 90°, FOV 24 × 24 cm, 64 × 64 matrix, 3.4 × 3.4 mm in-plane resolution, 5 mm slice thickness, 30 slices. Head motion was minimized using padding and restraint. During the 5-minute scan, participants were requested to look at the fixation cross hair and to keep eyes open. Participants were monitored by video.

2.3 Data analysis

2.3.1 Preprocessing—Functional MRI data were preprocessed using the SPM software package. The first four volumes are discarded to remove T1 equilibration effects. To correct residual head motion, "bad" images (confounded by motion or radio-frequency spikes) were estimated and removed using ART-Repair (Mazaika et al., 2007). These images were determined by calculating the mean intensity for a given time series and identifying individual images whose intensity was greater than four standard deviations from the mean. The offending image(s) were replaced in the time series by a rolling mean image, and regressed in the statistical model. Images were motion-corrected using INRIalign (Freire and

Mangin, 2001; Freire et al., 2002). Data were spatially normalized into the standard Montreal Neurological Institute space and resampled into 3 × 3 × 3 mm voxels, resulting in 53 × 63 × 46 voxels. Next, the data were spatially smoothed with a six mm full width at half-maximum Gaussian kernel. The MRI coordinates were converted to the Talairach and Tournoux standard space to assist with anatomical labeling. However, all (x,y,z) coordinates listed in the manuscript are in Montreal Neurological Institute (MNI), the default coordinate system in SPM.

2.3.2 Independent Component Analysis—Following preprocessing, a group independent component analysis (ICA) was performed in the complete sample (Calhoun et al., 2001; Calhoun and Adali, 2012). The methods were organized in batch scripts and performed via the group ICA of fMRI (GIFT) MATLAB toolbox version 1.3c (http://mialab.mrn.org/software/gift). FMRI time series data for all participants were first compressed through principal component analysis (PCA). There were two PCA data reduction stages, which reduced the impact of noise and makes the estimation computationally tractable (Calhoun et al., 2009; Erhardt et al., 2011; Schmithorst and Holland, 2004). The first data reduction stage was set to 45 components. The final dimensionality/number of components was 30. The data reduction was followed by a group spatial ICA, performed on the participants' aggregate data, resulting in the final estimation of our independent components (ICs) (Calhoun et al., 2001). The infomax algorithm was used, which attempts to minimize the mutual information of network outputs (Bell and Sejnowski, 1995). From the group spatial ICA, we reconstructed spatial maps and their corresponding ICA time courses that represented both the spatial and temporal characteristics of each component and subject using group ICA (GICA) (Erhardt et al., 2011). These maps and time courses were then inspected to determine which components reflected plausible non-artifact networks. ICs that depicted peak cluster locations in gray matter with minimal overlap with white matter, ventricles and edges of the brain and also exhibit higher low frequency temporal activity were retained for further analysis.

A larger ICA sample size would result in a better estimate of the resting-state networks, which would be better generalizable to the population of male juvenile delinquents. We therefore decided to perform our ICA in the larger sample, and to perform the Mancova analysis in the smaller, complete case sample.

2.3.3 Statistical analyses—Associations between psychopathy and functional connectivity were tested for complete cases only (n=177) using the Mancovan toolbox implemented in GIFT (Allen et al., 2011). We examined three connectivity measures: component spatial maps, component time course power spectra, and between component functional network connectivity (Jafri, Pearlson, Stevens, & Calhoun, 2008). The voxel intensity in the spatial map resembles the correspondence between a voxel time course and an IC time course (Balsters et al., 2013), thus providing a measure of a region's strength of connectivity within a given network. The time course power spectra reflect the degree of fluctuation in amplitude of the intrinsic activity within the network (Calhoun et al., 2011). The between component functional network connectivity represents correlations between the different components. Although ICs generated by ICA are maximally independent of each

other (Calhoun and Adali, 2006), their time courses can still exhibit temporal dependencies (Arbabshirani et al., 2013). A multivariate selection strategy was first performed in order to identify potential significant associations between component measures and variables of interest. FNC time courses were first despiked and temporally bandpass filtered (0.01 Hz-0.15 Hz) followed by calculation of the among network connectivity matrices. The initial design matrix included psychopathy scores, and age, IQ, ADHD diagnosis, and duration of alcohol and cannabis abuse, as covariates. In addition, we included head movement estimates as nuisance regressors (Allen et al., 2011), defined as the average of translation and rotation parameters. However, as results were similar with and without correction for head movement, we only report results of the model excluding motion parameters (motion corrected results are presented in Figures S4 t/m 9 and Table S2). Univariate analyses were performed within the reduced model (including only variables that showed significant associations in the multivariate stage) to test for specific relationships between predictors of interest and connectivity properties. An alpha level of 0.05 was used for all analyses. Associations between psychopathy and a priori networks of interest were first examined. For these region of interest analyses, we report both uncorrected and false discovery rate (FDR) corrected results (Genovese, Lazar, & Nichols, 2002). We then performed exploratory whole brain analyses, which were corrected for multiple comparisons using FDR.

3. Results

3.1 Group independent component analysis

We performed a 30 component GICA using resting-state fMRI data from 201 participants. Demographic information on the participants is provided in Table 1. Table 2 describes the correlations between the different variables in our model. Based on visual inspection of the spatial maps and power spectra, 15 components were identified as ventricular, vascular, susceptibility or motion-related artifacts (Figure S1). The 15 remaining components are shown in Figure S2 and coordinates of their peak activation are provided in Table S1. Figure S3 shows the functional network connectivity. The ICA parcellation resulted in similar networks as reports in typical samples (Beckmann et al., 2005; Calhoun et al., 2008). As the DMN (cingulate cortex), ECN 1 (orbitofrontal cortex) and SN (cingulate cortex) include paralimbic regions, functional connectivity parameters were examined in these networks prior to the whole brain analyses.

3.2 Component spatial maps

We found no associations between PCL-Total score and networks encompassing paralimbic regions. Consistent with hypotheses, the PCL Factor 1 score was associated with functional connectivity in regions of the SN ($p = 0.02$, uncorrected, Figure 1, Table 3). We found mostly negative associations in frontal, temporal and medial regions, suggesting that in these regions, there was a lower correspondence between voxel time course and SN time course with increasing Factor 1 scores. Additionally, Factor 1 scores were associated with spatial maps of the ECN ($p = 0.04$, uncorrected, Figure 2, Table 3), with negative associations in medial, temporal, parietal, and cerebellar regions of the left hemisphere, and positive associations in the bilateral thalamus, frontal, temporal, and cerebellar regions. Also for Factor 2 scores, association with the ECN spatial map were found ($p = 0.02$, uncorrected,

Figure 3, Table 3) in the insula, thalamus, and in frontal, temporal, and cerebellar regions. After correction for FDR, the whole-brain analyses did not provide any additional significant results.

3.3 Time course power spectra

The PCL Total Score was associated with increased amplitude at 0.0–0.05Hz and >0.2 Hz, and decreased amplitude at 0.05–0.1 Hz of the DMN ($p = 0.02$ uncorrected, Figure 4). This effect seems mostly driven by Factor 1 scores, as PCL factor 1, but not Factor 2, was associated with decreased low frequency power (0.0–0.1Hz) and increased high frequency power of the DMN (uncorrected $p = 0.03$, Figure 5a). Only the association in the higher frequencies survived correction for multiple comparisons (Figure 5b). After correction for FDR, the whole-brain analyses did not provide any additional significant results.

3.4 Functional network connectivity

There were no significant associations between FNC and PCL-YV scores.

4. Discussion

The present study examined the association between functional connectivity and psychopathic traits in a large sample of incarcerated adolescent boys. Based on prior structural and functional neuroimaging studies on psychopathy (for example Cope et al., 2014; De Brito et al., 2009; Ermer et al., 2013; Harenski et al., 2014; Kiehl et al., 2001; Pujol et al., 2012; Wallace et al., 2014; Yang et al., 2011), we hypothesized that psychopathic symptoms would be associated with aberrant functional connectivity within networks encompassing limbic and paralimbic brain regions. PCL-Total score and Factor 1 score were associated with increased high frequency power of the DMN. Moreover, we found mostly negative associations between PCL Factor 1 scores and spatial map of the SN in frontal, temporal and medial regions of the brain, while associations between Factor 1 and spatial maps of the ECN were both negative (left hemisphere) and positive (bilateral). PCL Factor 2 scores were associated with the spatial map of the ECN in the insula, thalamus, and in frontal, temporal, and cerebellar regions.

In line with previous studies examining the association between adult and adolescent psychopathy and functional connectivity (Cohn et al., 2015; Contreras-Rodriguez et al., 2015; Juarez et al., 2013; Motzkin et al., 2011; Philippi et al., 2015; Pujol et al., 2012), our results suggest that adolescent psychopathy total score and interpersonal and affective traits are associated with increased high frequency power of the DMN. As described above, the DMN is a task-negative network which has been implicated is self-referential thought, social perspective taking, future thought, and moral behavior (Andrews-Hanna, 2012). Since some of the core features of psychopathy involve self- and other referential processes, aberrant DMN activation may account for several psychopathy symptoms. For example, psychopaths are believed to have an inflated sense of self, with psychopaths often displaying egocentric and narcissistic behavior (Hare, 2003). Moreover, compared to healthy adults, psychopaths have impaired emotion recognition (social perspective taking) (Dawel et al., 2012), and show impaired performance on moral decision making tasks (Tassy et al., 2013).

Studies describing associations between psychopathy and DMN connectivity generally describe results in DMN spatial maps (e.g. Cohn et al., 2015) or discuss the temporal correlation between regions of the DMN (e.g. Pujol et al., 2012). When the co-activation of two regions is related to psychopathic traits, these regions are interpreted to function more or less independently with increasing psychopathic traits. The interpretation of associations in spatial maps are also relatively straight forward: in the larger sample, each network comprises of a specific set of voxels, however, for individuals with more or less psychopathic traits, certain voxels or regions may be more or less involved. The origin of rs-fMRI spectral power at different frequencies currently is less well understood. Moreover, the lack of a particular task makes it difficult to characterize different brain processes across multiple subjects. The MR signal is dominated by oscillations in the 0.0–0.1 Hz frequency band. Our results suggest that psychopathic traits are associated with increased high frequency (>0.1 Hz) power. Although high frequency oscillations are often discarded due to their susceptibility to physiological noise, several studies have shown associations between higher frequency oscillations and psychiatric disorders, such as attention deficit hyperactivity disorder and depression (Yu et al., 2016; Yue et al., 2015). As our results in the DMN withstood correction for motion parameters, we believe it is unlikely that the effect in DMN power spectra could be (completely) ascribed to increased motion in participants with increased psychopathic traits. Instead, youth with increased psychopathic traits may display a less coherent pattern of DMN activation.

In addition to increased DMN high frequency power, adolescent interpersonal and affective traits were associated with the spatial map of the SN. The SN, which encompasses the insula and the ACC as well as the amygdala, has been implicated in assigning emotional attributes and salience to external and internal stimuli, and integrates this information to influence behavior (Menon and Uddin, 2010). Indeed, several event-related potential oddball studies have reported aberrant processing of salient stimuli in psychopathic individuals (Anderson et al., 2015; Kiehl et al., 1999). Moreover, neuroimaging studies have repeatedly reported associations between psychopathy and ACC, insula, and amygdala structure and functioning, both during tasks and at rest. For example, compared to non-psychopathic inmates, psychopathic inmates have been reported to show reduced insula and ACC thickness as well a corresponding reduction in functional connectivity (Ly et al., 2012). In a study on resting state connectivity in adult psychopaths, functional connectivity of the SN was negatively associated with Factor 1 scores, but positively associated with Factor 2 scores (Philippi et al., 2015). Moreover, compared to inmates scoring low on psychopathy, psychopathic inmates showed decreased connectivity between the amygdala or temporoparietal junction and regions of the SN while watching moral images (Yoder et al., 2015).

Both interpersonal and affective traits and lifestyle and antisocial traits were associated with the spatial map of the ECN. In our data, the ECN largely comprises of the OFC and inferior frontal cortex. Several studies have suggested that psychopathy is associated with specific executive functions ascribed to OFC functioning (Blair et al., 2006; Lantrip et al., 2016; Lapierre et al., 1995). Although we do not report associations in the OFC per se, the associations between antisocial traits and ECN spatial map may provide support for OFC network dysfunction in psychopathy. Moreover, comparable to our results, Cohn et al. (2015) report associations between psychopathic impulsive and irresponsible traits—but not

callous and unemotional, or grandiose-manipulative traits—and spatial map of a cognitive control network.

In his triple network model, Menon (2011) argues that deficits in the (dis)engagement of the DMN, SN, and fronto-parietal network may play a role in many psychiatric and neurological disorders. In this model, the SN plays a role in saliency detection, attentional capture and dynamic cognitive control. In case of a salient event, the SN may initiate network switching, leading to engagement of the fronto-parietal network (cognition) and disengagement of the DMN (rest). An important aspect of the model in explaining psychopathology is the inappropriate assignment of saliency to external or internal stimuli carried out by the SN. Here, we report small effects of psychopathy in both SN and DMN functional connectivity, and also report associations between psychopathy and a network involved in cognition, providing some evidence for the triple network model in psychopathy.

Although the DMN and the salience/cingulo-opercular network have been implicated in adult Factor 2 traits (Philippi et al., 2015), the present study did not provide evidence for an association between DMN and SN functional connectivity and Factor 2 scores in adolescents. This suggests that associations between the DMN and SN and Factor 2 scores may develop later in life. These differences in functional connectivity may reflect a consequence of psychopathic antisocial traits rather than a cause of psychopathy. Moreover, the different findings for Factor 1 scores and Factor 2 scores suggest that treatment and prevention strategies for psychopathy may benefit from targeting Factor 1 and Factor 2 traits separately.

We did not find associations between psychopathic traits and FNC. FNC describes the co-activation of the different functional networks. Although several networks encompassing paralimbic regions are associated with psychopathic traits, psychopathy seems unrelated to between-network communication.

While psychopaths have been deemed untreatable, recent research shows that especially juveniles may be susceptible to treatment efforts. Instead of punishing unwanted behavior as is common in juvenile facilities, psychopaths seem to benefit from positive reinforcement (Caldwell et al., 2007; Kiehl and Hoffman, 2011). As our results as well as the results of other studies suggest aberrant functioning of the DMN, mindfulness meditation may also be a viable treatment option for youth with elevated psychopathic traits. Mindfulness meditation has been shown to increase functional connectivity of the DMN (Creswell et al., 2016). Moreover, mindfulness has been suggested to play a role in antisocial personality disorder (Fossati et al., 2012; Velotti et al., 2016). Future studies may want to examine the effect of mindfulness training on psychopathic behavior.

Some limitations should be noted. The present sample contains only males. Due to the many differences between males and females in psychopathic traits and brain structure and functioning, and neural development (Mutlu et al., 2013; Strand and Belfrage, 2005; Wang et al., 2008), we believe it is a good strategy to examine males and females separately. However, future research should examine whether these effects also apply to female samples. Except for the association between interpersonal and affective traits and DMN

power spectra, our results did not survive FDR correction for multiple testing, and should thus be interpreted with caution.

In conclusion, the present study examined the association between adolescent psychopathic traits and resting-state functional connectivity in a large sample of juvenile delinquents. As comparable to studies in adults, we found associations between interpersonal and affective traits and properties of the DMN, SN, and ECN. Lifestyle and antisocial traits were associated with the ECN. These networks have been implicated in self-referential thought, moral behavior, saliency detection, and executive functioning: functions which are reported to be disrupted in psychopaths. As these networks encompass limbic and paralimbic brain regions, the present study provides evidence for paralimbic system dysfunction in psychopathy.

Supplementary Material

Refer to Web version on PubMed Central for supplementary material.

Acknowledgments

Data collection was funded by NIMH; 1 R01 MH071896-01 (PI: Kent A. Kiehl) and NICHD: 1R01HD082257-01 (PI: Kent A. Kiehl). Sandra Thijssen was supported by a European Research Council grant (ERC AdG 669249) awarded to Marian J. Bakermans-Kranenburg.

References

Aertsen AMHJ, Gerstein GL, Habib MK, Palm G. Dynamics of neuronal firing correlation - modulation of effective connectivity. J Neurophysiol. 1989; 61(5):900–917. [PubMed: 2723733]

Aghajani M, Colins OF, Klapwijk ET, Veer IM, Andershed H, Popma A, Vermeiren RRJM. Dissociable relations between amygdala subregional networks and psychopathy trait dimensions in conduct-disordered juvenile offenders. Hum Brain Mapp. 2016; 37(11):4017–4033. DOI: 10.1002/hbm.23292 [PubMed: 27453465]

Allen EA, Erhardt EB, Damaraju E, Gruner W, Segall JM, Silva RF, Calhoun VD. A baseline for the multivariate comparison of resting-state networks. Front Syst Neurosci. 2011; 5(2)doi: 10.3389/fnsys.2011.00002

Anderson NE, Steele VR, Maurer JM, Bernat EM, Kiehl KA. Psychopathy, attention, and oddball target detection: New insights from PCL-R facet scores. Psychophysiology. 2015; 52(9):1194–1204. DOI: 10.1111/psyp.12441 [PubMed: 25912522]

Andrews-Hanna JR. The brain's default network and its adaptive role in internal mentation. Neuroscientist. 2012; 18(3):251–270. DOI: 10.1177/1073858411403316 [PubMed: 21677128]

Arbabshirani MR, Havlicek M, Kiehl KA, Pearlson GD, Calhoun VD. Functional network connectivity during rest and task conditions: a comparative study. Hum Brain Mapp. 2013; 34(11):2959–2971. DOI: 10.1002/hbm.22118 [PubMed: 22736522]

Balsters JH, O'Connell RG, Galli A, Nolan H, Greco E, Kilcullen SM, Robertson IH. Changes in resting connectivity with age: a simultaneous electroencephalogram and functional magnetic resonance imaging investigation. Neurobiol Aging. 2013; 34(9):2194–2207. DOI: 10.1016/j.neurobiolaging.2013.03.004 [PubMed: 23608113]

Beckmann CF, DeLuca M, Devlin JT, Smith SM. Investigations into resting-state connectivity using independent component analysis. Philos T R Soc B. 2005; 360(1457):1001–1013. DOI: 10.1098/rstb.2005.1634

Bell AJ, Sejnowski TJ. An information maximization approach to blind separation and blind deconvolution. Neural Comput. 1995; 7(6):1129–1159. DOI: 10.1162/neco.1995.7.6.1129 [PubMed: 7584893]

Blair KS, Newman C, Mitchell DGV, Richell RA, Leonard A, Morton J, Blair RJR. Differentiating among prefrontal substrates in psychopathy: Neuropsychological test findings. Neuropsychol. 2006; 20(2):153–165. DOI: 10.1037/0894-4105.20.2.153

Broulidakis MJ, Fairchild G, Sully K, Blumensath T, Darekar A, Sonuga-Barke EJS. Reduced default mode connectivity in adolescents with conduct disorder. J Am Acad Child Psy. 2016; 55(9):800–808. DOI: 10.1016/j.jaac.2016.05.021

Buckner RL, Andrews-Hanna JR, Schacter DL. The brain's default network - Anatomy, function, and relevance to disease. Ann Ny Acad Sci. 2008; 1124:1–38. DOI: 10.1196/annals.1440.011 [PubMed: 18400922]

Caldwell MF, McCormick DJ, Umstead D, Van Rybroek GJ. Evidence of treatment progress and therapeutic outcomes among adolescents with psychopathic features. Crim Justice Behav. 2007; 34(5):573–587. DOI: 10.1177/0093854806297511

Calhoun V, Adali T, Pearlson G, Pekar J. A method for making group inferences using independent component analysis of functional MRI data: Exploring the visual system. Neuroimage. 2001; 13(6):S88–S88.

Calhoun VD, Adali T. Unmixing fMRI with independent component analysis. IEEE Eng Med Biol Mag. 2006; 25(2):79–90.

Calhoun VD, Adali T. Multisubject independent component analysis of fMRI: a decade of intrinsic networks, default mode, and neurodiagnostic discovery. IEEE Rev Biomed Eng. 2012; 5:60–73. DOI: 10.1109/RBME.2012.2211076 [PubMed: 23231989]

Calhoun VD, Kiehl KA, Pearlson GD. Modulation of temporally coherent brain networks estimated using ICA at rest and during cognitive tasks. Hum Brain Mapp. 2008; 29(7):828–838. DOI: 10.1002/HumBrainMapp.20581 [PubMed: 18438867]

Calhoun VD, Liu J, Adali T. A review of group ICA for fMRI data and ICA for joint inference of imaging, genetic, and ERP data. Neuroimage. 2009; 45(1):S163–S172. DOI: 10.1016/j.neuroimage.2008.10.057 [PubMed: 19059344]

Calhoun VD, Sui J, Kiehl K, Turner J, Allen E, Pearlson G. Exploring the psychosis functional connectome: aberrant intrinsic networks in schizophrenia and bipolar disorder. Front Psychiat. 2011; 2:75.doi: 10.3389/fpsyt.2011.00075

Cerliani L, Mennes M, Thomas RM, Di Martino A, Thioux M, Keysers C. Increased functional connectivity between subcortical and cortical resting-state networks in autism spectrum disorder. Jama Psychiat. 2015; 72(8):767–777. DOI: 10.1001/jamapsychiatry.2015.0101

Cohn MD, Pape LE, Schmaal L, van den Brink W, van Wingen G, Vermeiren RRJM, Popma A. Differential relations between juvenile psychopathic traits and resting state network connectivity. Hum Brain Mapp. 2015; 36(6):2396–2405. DOI: 10.1002/hbm.22779 [PubMed: 25757797]

Contreras-Rodriguez O, Pujol J, Batalla I, Harrison BJ, Bosque J, Ibern-Regas I, Cardoner N. Disrupted neural processing of emotional faces in psychopathy. Soc Cogn Affect Neur. 2014; 9(4):505–512. DOI: 10.1093/scan/nst014

Contreras-Rodriguez O, Pujol J, Batalla I, Harrison BJ, Soriano-Mas C, Deus J, Cardoner N. Functional connectivity bias in the prefrontal cortex of psychopaths. Biol Psychiat. 2015; 78(9):647–655. DOI: 10.1016/j.biopsych.2014.03.007 [PubMed: 24742618]

Cope LM, Ermer E, Nyalakanti PK, Calhoun VD, Kiehl KA. Paralimbic gray matter reductions in incarcerated adolescent females with psychopathic traits. J Abnorm Child Psych. 2014; 42(4):659–668. DOI: 10.1007/s10802-013-9810-4

Creswell JD, Taren AA, Lindsay EK, Greco CM, Gianaros AF, Marsland AL, Ferris JL. Alterations in resting state functional connectivity link mindfulness meditation with reduced interleukin-g: A randomized controlled trial. Biol Psychiat. 2016; 80(1):53–61. [PubMed: 27021514]

Dawel A, O'Kearney R, McKone E, Palermo R. Not just fear and sadness: Meta-analytic evidence of pervasive emotion recognition deficits for facial and vocal expressions in psychopathy. Neurosci Biobehav R. 2012; 36(10):2288–2304. DOI: 10.1016/j.neubiorev.2012.08.006

De Brito SA, Mechelli A, Wilke M, Laurens KR, Jones AP, Barker GJ, Viding E. Size matters: Increased grey matter in boys with conduct problems and callousunemotional traits. Brain. 2009; 132:843–852. DOI: 10.1093/Brain/Awp011 [PubMed: 19293245]

Decety J, Skelly L, Yoder KJ, Kiehl KA. Neural processing of dynamic emotional facial expressions in psychopaths. Soc Neurosci. 2014; 9(1):36–49. DOI: 10.1080/17470919.2013.866905 [PubMed: 24359488]

Erhardt EB, Rachakonda S, Bedrick EJ, Allen EA, Adali T, Calhoun VD. Comparison of multi-subject ICA methods for analysis of fMRI data. Hum Brain Mapp. 2011; 32(12):2075–2095. DOI: 10.1002/hbm.21170 [PubMed: 21162045]

Ermer E, Cope LM, Nyalakanti PK, Calhoun VD, Kiehl KA. Aberrant para limbic gray matter in incarcerated male adolescents with psychopathic traits. J Am Acad Child Psy. 2013; 52(1):94–103. DOI: 10.1016/j.jaac.2012.10.013

Forth, AE., Kosson, D., Hare, RD. The Hare Psychopathy Checklist: Youth Version. New York: Multi-Health Systems; 2003.

Fossati A, Porro FV, Maffei C, Borroni S. Are the dsm-iv personality disorders related to mindfulness? An italian study on clinical participants. J Clin Psychol. 2012; 68(6):672–683. DOI: 10.1002/jclp.21848 [PubMed: 22517635]

Freire L, Mangin JF. Motion correction algorithms may create spurious brain activations in the absence of subject motion. Neuroimage. 2001; 14(3):709–722. DOI: 10.1006/nimg.2001.0869 [PubMed: 11506543]

Freire L, Roche A, Mangin JF. What is the best similarity measure for motion correction in fMRI time series? IEEE T Med Imaging. 2002; 21(5):470–484. DOI: 10.1109/Tmi.2002.1009383

Genovese CR, Lazar NA, Nichols T. Thresholding of statistical maps in functional neuroimaging using the false discovery rate. Neuroimage. 2002; 15(4):870–878. DOI: 10.1006/nimg.2001.1037 [PubMed: 11906227]

Gogtay N, Giedd JN, Lusk L, Hayashi KM, Greenstein D, Vaituzis AC, Thompson PM. Dynamic mapping of human cortical development during childhood through early adulthood. P Natl Acad Sci USA. 2004; 101(21):8174–8179. DOI: 10.1073/pnas.0402680101

Gregory S, Ffytche D, Simmons A, Kumari V, Howard M, Hodgins S, Blackwood N. The antisocial brain: psychopathy matters a structural mri investigation of antisocial male violent offenders. Arch Gen Psychiat. 2012; 69(9):962–972. DOI: 10.1001/archgenpsychiatry.2012.222 [PubMed: 22566562]

Hare, RD. Manual for the Hare Psychopathy Checklist-Revised. Toronto: Multi-Health Systems; 2003.

Harenski CL, Harenski KA, Kiehl KA. Neural processing of moral violations among incarcerated adolescents with psychopathic traits. Dev Cogn Neurosci. 2014; 10:181–189. DOI: 10.1016/j.dcn.2014.09.002 [PubMed: 25279855]

Harenski CL, Harenski KA, Shane MS, Kiehl KA. Aberrant neural processing of moral violations in criminal psychopaths. J Abnorm Psychol. 2010; 119(4):863–874. DOI: 10.1037/a0020979 [PubMed: 21090881]

Hemphill JF, Templeman R, Wong S, Hare RD. Psychopathy and crime: Recidivism and criminal careers. Nato Adv Sci I D-Beh. 1998; 88:375–399.

Jafri MJ, Pearlson GD, Stevens M, Calhoun VD. A method for functional network connectivity among spatially independent resting-state components in schizophrenia. Neuroimage. 2008; 39(4):1666–1681. DOI: 10.1016/j.neuroimage.2007.11.001 [PubMed: 18082428]

Juarez M, Kiehl KA, Calhoun VD. Intrinsic limbic and paralimbic networks are associated with criminal psychopathy. Hum Brain Mapp. 2013; 34(8):1921–1930. DOI: 10.1002/Hbm.22037 [PubMed: 22431294]

Kaufman J, Birmaher B, Brent D, Rao U, Flynn C, Moreci P, Ryan N. Schedule for Affective Disorders and Schizophrenia for School-Age Children Present and Lifetime version (K-SADS-PL): Initial reliability and validity data. J Am Acad Child Psy. 1997; 36(7):980–988. DOI: 10.1097/00004583-199707000-00021

Kiehl KA. A cognitive neuroscience perspective on psychopathy: Evidence for paralimbic system dysfunction. Psychiat Res. 2006; 142(2–3):107–128. DOI: 10.1016/j.psychres.2005.09.013

Kiehl KA, Hare RD, Liddle PF, McDonald JJ. Reduced P300 responses in criminal psychopaths during a visual oddball task. Biol Psychiat. 1999; 45(11):1498–1507. DOI: 10.1016/S0006-3223(9800193-0 [PubMed: 10356633]

Kiehl KA, Hoffman MB. The criminal psychopath: history, neuroscience, treatment, and economics. Jurimetrics. 2011; 51:355–397. [PubMed: 24944437]

Kiehl KA, Smith AM, Hare RD, Mendrek A, Forster BB, Brink J, Liddle PF. Limbic abnormalities in affective processing by criminal psychopaths as revealed by functional magnetic resonance imaging. Biol Psychiat. 2001; 50(9):677–684. DOI: 10.1016/S0006-3223(0101222-7 [PubMed: 11704074]

Lantrip C, Towns S, Roth RM, Giancola PR. Psychopathy traits are associated with self-report rating of executive functions in the everyday life of healthy adults. Pers Indiv Differ. 2016; 101:127–131. DOI: 10.1016/j.paid.2016.05.051

Lapierre D, Braun CMJ, Hodgins S. Ventral frontal deficits in psychopathy - neuropsychological test findings. Neuropsychologia. 1995; 33(8):1059–1059.

Li WQ, Mai XQ, Liu C. The default mode network and social understanding of others: what do brain connectivity studies tell us. Front Hum Neurosci. 2014; 8 doi: ARTN 74 10.3389/fnhum.2014.00074.

Ly M, Motzkin JC, Philippi CL, Kirk GR, Newman JP, Kiehl KA, Koenigs M. Cortical thinning in psychopathy. Am J Psychiat. 2012; 169(7):743–749. DOI: 10.1176/appi.ajp.2012.11111627 [PubMed: 22581200]

Marsh AA, Cardinale EM. When psychopathy impairs moral judgments: neural responses during judgments about causing fear. Soc Cogn Affect Neurosci. 2014; 9(1):3–11. DOI: 10.1093/scan/nss097 [PubMed: 22956667]

Menon V. Large-scale brain networks and psychopathology: a unifying triple network model. Trends Cogn Sci. 2011; 15(10):483–506. DOI: 10.1016/j.tics.2011.08.003 [PubMed: 21908230]

Menon V, Uddin LQ. Saliency, switching, attention and control: a network model of insula function. Brain Struct Funct. 2010; 214(5–6):655–667. DOI: 10.1007/s00429-010-0262-0 [PubMed: 20512370]

Motzkin JC, Newman JP, Kiehl KA, Koenigs M. Reduced prefrontal connectivity in psychopathy. J Neurosci. 2011; 31(48):17348–17357. DOI: 10.1523/Jneurosci.4215-11.2011 [PubMed: 22131397]

Mutlu AK, Schneider M, Debbane M, Badoud D, Eliez S, Schaer M. Sex differences in thickness, and folding developments throughout the cortex. Neuroimage. 2013; 82:200–207. DOI: 10.1016/j.neuroimage.2013.05.076 [PubMed: 23721724]

Philippi CL, Pujara MS, Motzkin JC, Newman J, Kiehl KA, Koenigs M. Altered resting-state functional connectivity in cortical networks in psychopathy. J Neurosci. 2015; 35(15):6068–6078. DOI: 10.1523/Jneurosci.5010-14.2015 [PubMed: 25878280]

Pujol J, Batalla I, Contreras-Rodriguez O, Harrison BJ, Pera V, Hernandez-Ribas R, Cardoner N. Breakdown in the brain network subserving moral judgment in 25 criminal psychopathy. Soc Cogn Affect Neurosci. 2012; 7(8):917–923. DOI: 10.1093/Scan/Nsr075 [PubMed: 22037688]

Rashid B, Damaraju E, Pearlson GD, Calhoun VD. Dynamic connectivity states estimated from resting fMRI Identify differences among schizophrenia, bipolar disorder, and healthy control subjects. Front Hum Neurosci. 2014; 8 doi: Artn 89710.3389/Fnhum.2014.00897.

Rogers BP, Morgan VL, Newton AT, Gore JC. Assessing functional connectivity in the human brain by fMRI. Magnet Reson Imaging. 2008; 26(1):146–146. DOI: 10.1016/j.mri.2007.06.002

Schmithorst VJ, Holland SK. Comparison of three methods for generating group statistical inferences from independent component analysis of functional magnetic resonance imaging data. J Magnet Reson Im. 2004; 19(3):365–368. DOI: 10.1002/Jmri.20009

Shannon BJ, Raichle ME, Snyder AZ, Fair DA, Mills KL, Zhang DY, Kiehl KA. Premotor functional connectivity predicts impulsivity in juvenile offenders. P Natl Acad Sci USA. 2011; 108(27):11241–11245. DOI: 10.1073/pnas.1108241108

Sheng T, Gheytanchi A, Aziz-Zadeh L. Default network deactivations are correlated with psychopathic personality traits. Plos One. 2010; 5(9) doi: ARTN e12611 10.1371/journal.pone.0012611.

Strand S, Belfrage H. Gender differences in psychopathy in a Swedish offender sample. Behav Sci Law. 2005; 23(6):837–850. DOI: 10.1002/bsl.674 [PubMed: 16333809]

Tassy S, Deruelle C, Mancini J, Leistedt S, Wicker B. High levels of psychopathic traits alters moral choice but not moral judgment. Front Hum Neurosci. 2013; 7 doi: Artn 22910.3389/Fnhum.2013.00229.

Velotti P, Garofalo C, D'Aguanno M, Petrocchi C, Popolo R, Salvatore G, Dimaggio G. Mindfulness moderates the relationship between aggression and Antisocial Personality Disorder traits: Preliminary investigation with an offender sample. Compr Psychiat. 2016; 64:38–45. DOI: 10.1016/j.comppsych.2015.08.004 [PubMed: 26350275]

Viding E, Blair RJR, Moffitt TE, Plomin R. Evidence for substantial genetic risk for psychopathy in 7-year-olds. J Child Psychol Psyc. 2005; 46(6):592–597. DOI: 10.1111/j.1469-7610.2004.00393.x

Wallace GL, White SF, Robustelli B, Sinclair S, Hwang S, Martin A, Blair RJR. Cortical and subcortical abnormalities in youths with conduct disorder and elevated callous-unemotional traits. J Am Acad Child Psy. 2014; 53(4):456–465. DOI: 10.1016/j.jaac.2013.12.008

Wang, L., Zhu, C., He, Y., Zhong, Q., Zang, Y. Gender Effect on Functional Networks in Resting Brain. In: Gao, X.Müller, H.Loomes, MJ.Comley, R., Luo, S., editors. Medical Imaging and Informatics: 2nd International Conference, MIMI, 2007; Beijing, China. August 14–16, 2007; Berlin, Heidelberg: Springer Berlin Heidelberg; 2008. Revised Selected Papers, 160-168

Wechsler, D. Wechsler Adult Intelligence Scale. New York: Psychological Corporation; 1997.

Wechsler, D. Wechlser Intelligence Scale for Children. Fourth. San Antonio, TX: Psychological Corporation; 2003.

Yang YL, Raine A, Colletti P, Toga AW, Narr KL. Abnormal structural correlates of response perseveration in individuals with psychopathy. J Neuropsych Clin N. 2011; 23(1):107–110. DOI: 10.1176/appi.neuropsych.23.1.107

Yang YL, Raine A, Lencz T, Bihrle S, LaCasse L, Colletti P. Volume reduction in prefrontal gray matter in unsuccessful criminal psychopaths. Biol Psychiat. 2005; 57(10):1103–1108. DOI: 10.1016/j.biopsych.2005.01.021 [PubMed: 15866549]

Yoder KJ, Harenski C, Kiehl KA, Decety J. Neural networks underlying implicit and explicit moral evaluations in psychopathy. Transl Psychiat. 2015; 5:e625. doi: tp2015117 [pii] 10.1038/tp.2015.117.

Yu XY, Yuan BK, Cao QJ, An L, Wang P, Vance A, Sun L. Frequency-specific abnormalities in regional homogeneity among children with attention deficit hyperactivity disorder: a resting-state fMRI study. Sci Bull. 2016; 61(9):682–692. DOI: 10.1007/s11434-015-0823-y

Yue YY, Jia XZ, Hou ZH, Zang YF, Yuan YG. Frequency-dependent amplitude alterations of resting-state spontaneous fluctuations in late-onset depression. Biomed Res Int. 2015 505479 doi: Artn 505479 10.1155/2015/505479.

Author Manuscript

Author Manuscript

Author Manuscript

Highlights

- Adolescent psychopathic traits are associated with default mode network power spectra
- Factor 1 scores correlate with salient and executive control network spatial maps
- Adolescent Factor 2 scores are associated executive control network spatial map

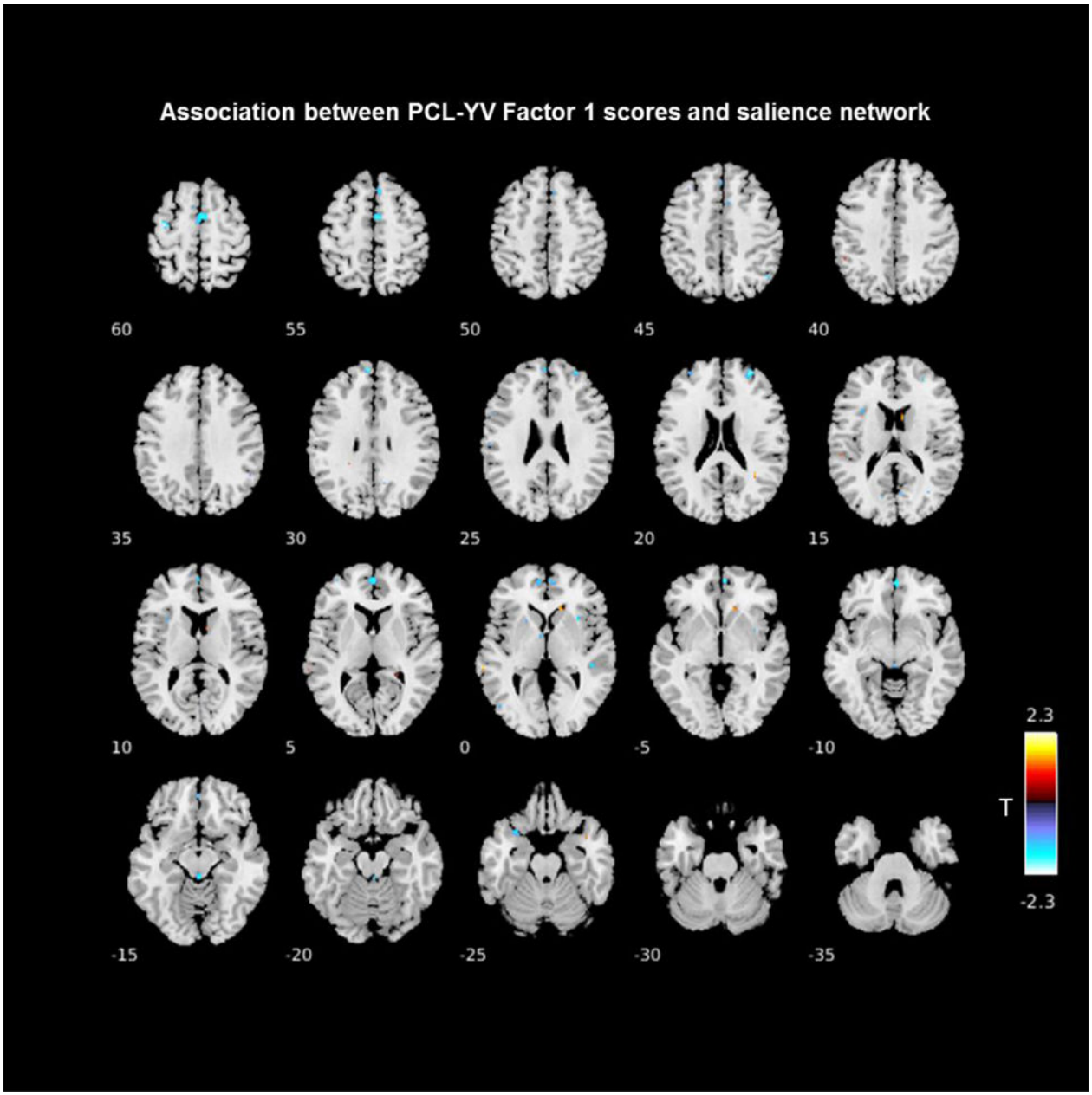

Figure 1.
Association between PCL-YV Factor 1 and spatial map of the salience network, $p < 0.05$

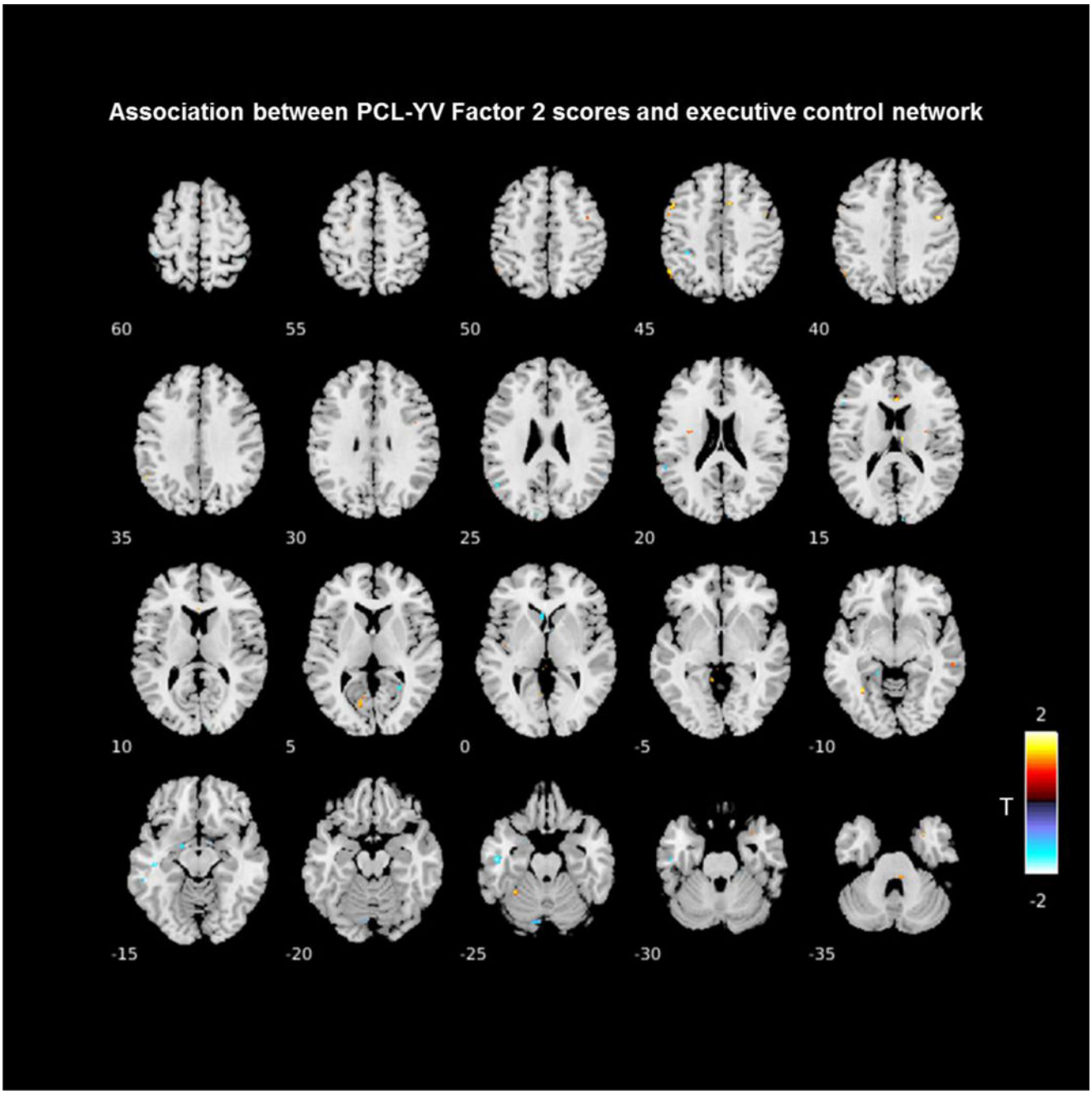

Figure 2.

Association between PCL-YV Factor 1 and spatial map of the executive control network, $p < 0.05$

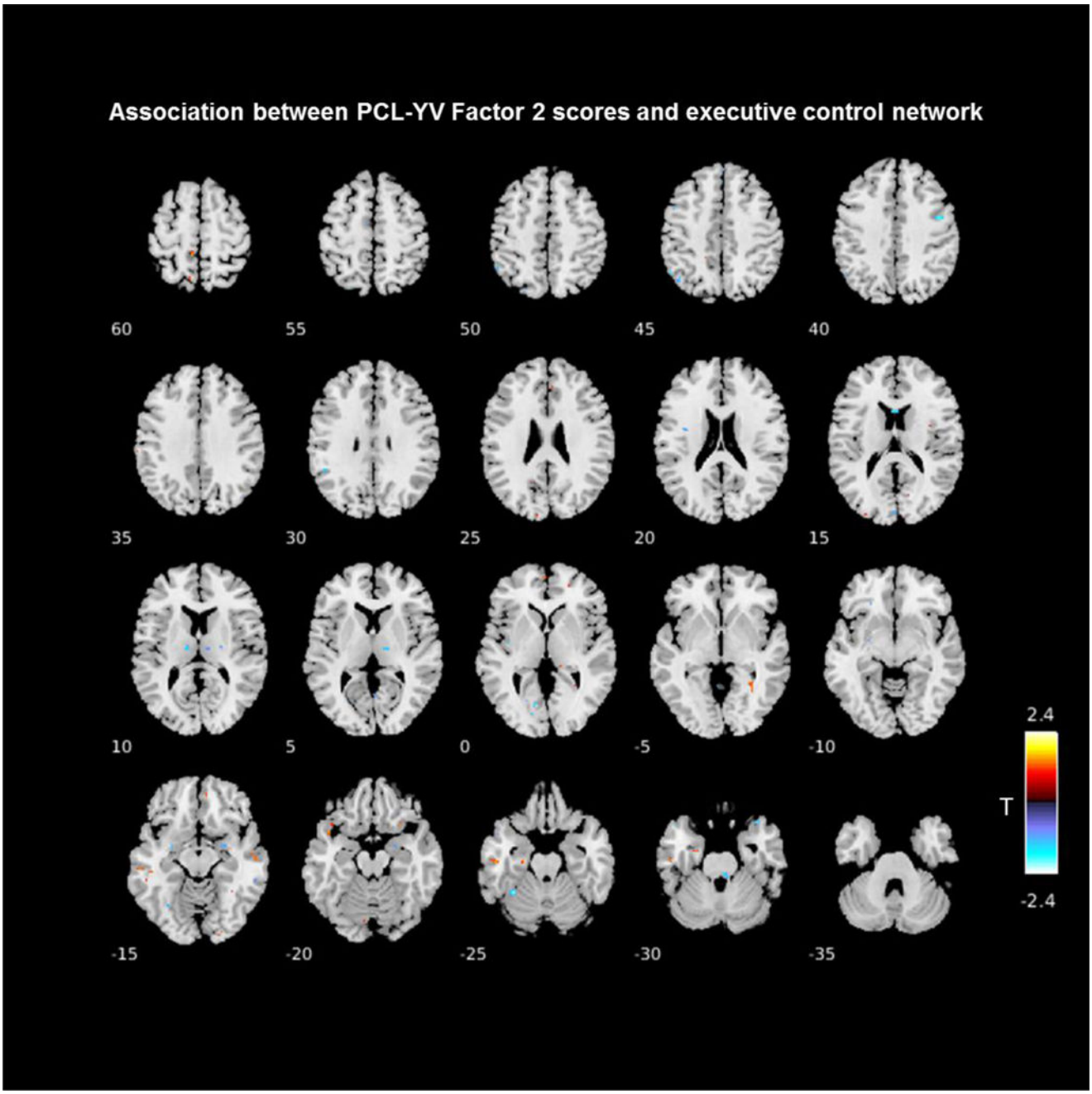

Figure 3.
Association between PCL-YV Factor 2 and spatial map of the executive control network, $p < 0.05$

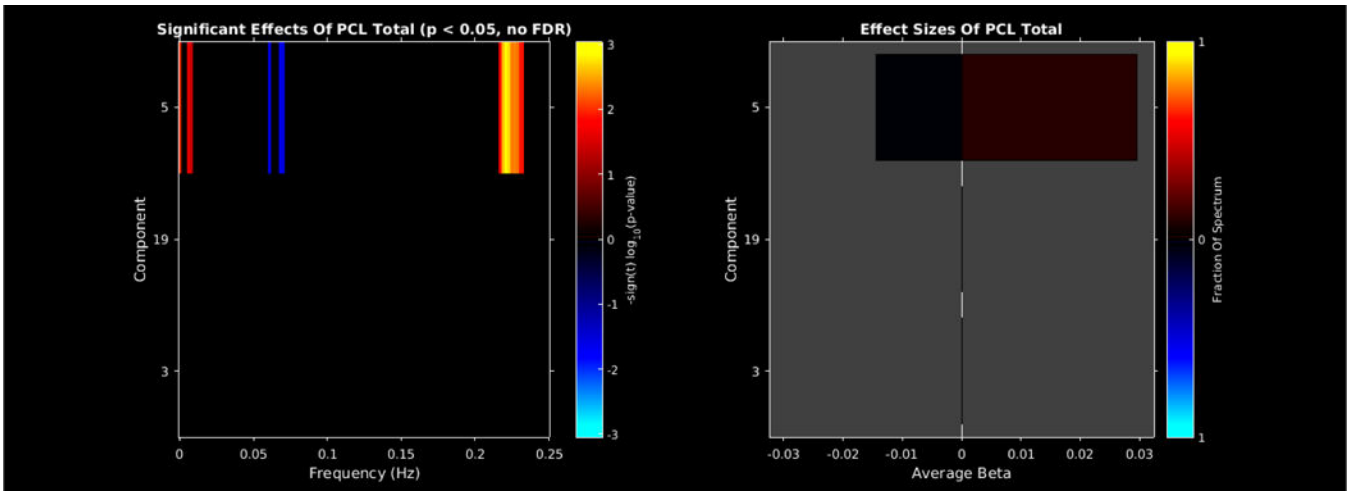

Figure 4.

Association between PCL-YV Total score and power spectra of the default mode network. Univariate tests were performed only on covariates of interest retained in the reduced MANCOVA model. Left panel depicts the significance and direction of PCL-YV Total score as a function of frequency for each component, displayed as - $sign(t)log_{10}(p)$. Right panel shows bar plots of the average β-values for PCL-YV Total score term. β-Values were averaged over frequency bands with effects of the same directionality. The color of the bar is proportional to the fraction of contributing frequency bins; the absence of a bar indicates that either univariate tests were not performed or test statistics were not significant.

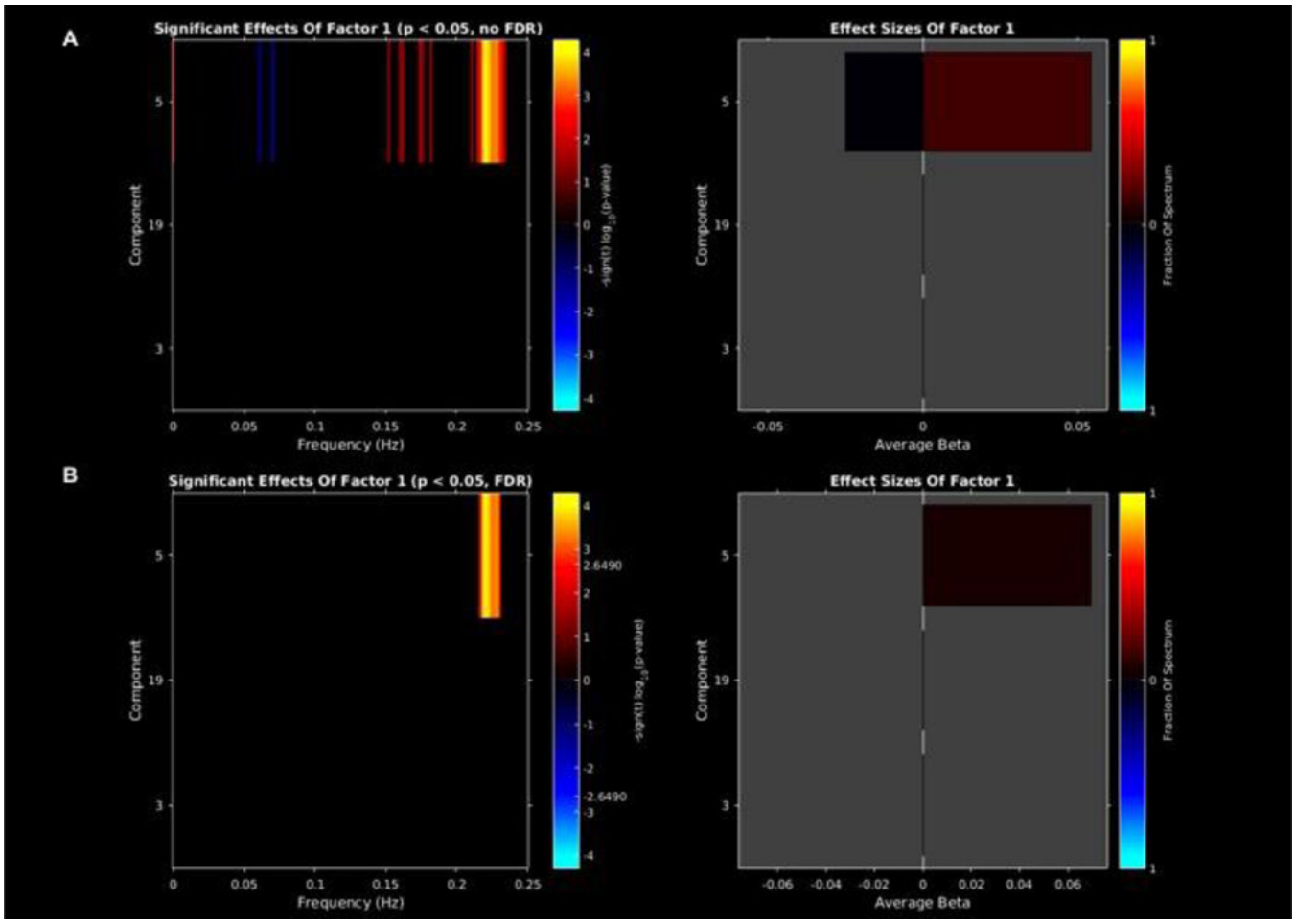

Figure 5.

Association between PCL-YV Factor 1 score and power spectra of the default mode network (A. no FDR correction, B. FDR corrected). Univariate tests were performed only on covariates of interest retained in the reduced MANCOVA model. Left panel depicts the significance and direction of PCL-YV Factor 1 as a function of frequency for each component, displayed as - $sign(t)log_{10}(p)$. Right panel shows bar plots of the average β-values for PCL-YV Factor 1 term. β-Values were averaged over frequency bands with effects of the same directionality where test statistics exceeded the FDR threshold. The color of the bar is proportional to the fraction of contributing frequency bins; the absence of a bar indicates that either univariate tests were not performed or test statistics were not significant.

Table 1

Sample characteristics

	n	*M*(*SD*)/n(%)	*M*(*SD*)/n(%) complete cases (n=177)	Min	Max
Age	201	17.19 (1.14)	17.18 (1.14)	14.08	18.92
IQ	168	90.56 (13.22)	90.71 (13.67)	54	140
Handedness	161				
Left		18 (11.2)	15 (10.27)		
Right		143 (88.2)	126 (87.67)		
ADHD	196	43 (21.94)	40 (22.60)		
Cannabis dependent	181	130 (71.8)	118 (71.42)		
Duration of cannabis use (months)	196	42.83 (31.37)	42.14 (31.73)	0.00	122.00
Alcohol dependent	181	96 (53.0)	89 (53.94)		
Duration of alcohol use (months)	198	23.06 (28.19)	20.77 (26.73)	0.00	120.00
PCL-YV	201				
Total scores		25.02 (6.15)	25.00 (6.16)	7.80	38.00
Factor 1		7.49 (3.29)	7.43 (3.22)	0.00	16.00
Factor 2		15.10 (2.89)	15.11 (2.90)	6.00	20.00

Table 2

Correlation table

	PCL F1	PCL F2	Age	IQ	Duration of cannabis use	Duration of alcohol use	ADHD
PCL Total	0.89***	0.87***	−0.15*	−0.12	0.17*	0.11	0.19*
PCL F1	1.00	0.60***	−0.13	−0.06	0.08	0.06	0.21**
PCL F2		1.00	−0.14	−0.13	0.24**	0.13	0.12
Age			1.00	0.17*	0.21**	0.24***	−0.25**
IQ				1.00	0.15*	0.23**	0.01
Duration of cannabis use					1.00	0.45***	−0.12
Duration alcohol use						1.00	0.03

Note.

*$p < 0.05$

**$p < 0.01$

***$p < 0.001$.

Table 3

Association between PCL-YV Factor scores and network spatial maps

Region	Hemisphere	*Max T*	MNI coordinates x,y,z
Factor 1 association with spatial maps of salience network - negative effects			
Middle Frontal Gyrus	L	2.4	−36, −6, 60
	R	2.6	33, 57, 24
Superior Temporal Gyrus	L	2.4	−33, 12, −24
	R	2.0	51, −33, 3
Medial Frontal Gyrus	R	2.4	3, 51, −12
Superior Frontal Gyrus	L	2.2	−3, 60, 27
	R	2.4	9, 27, 54
Postcentral Gyrus	L	2.3	−60, −18, 24
Precentral Gyrus	L	2.1	−33, −9, 60
Precuneus	R	2.0	12, −60, 33
Factor 1 association with spatial maps of salience network - positive effects			
Superior Temporal Gyrus	L	2.3	−63, −30, 6
Sub-Gyral	R	2.3	36, −51, 18
Caudate	R	2.2	9, 6, 12
Superior Frontal Gyrus	R	2.0	3, 51, 36
Factor 1 association with spatial maps of executive control network - negative effects			
Declive	L	2.5	−15, −84, −24
Sub-Gyral	L	2.4	−48, −27, −12
Inferior Parietal Lobule	L	2.3	−45, −39, 57
Cingulate Gyrus	L	2.3	0, 12, 33
Paracentral Lobule	L	2.2	−3, −39, 69
Cuneus	L	2.2	−9, −93, 27
	R	2.2	9, −99, 15
Uncus	L	2.1	−24, 3, −24
Middle Temporal Gyrus	L	2.1	−63, −42, −12
Inferior Temporal Gyrus	L	2.1	−51, −18, −27
Factor 1 association with spatial maps of executive control network - negative effects			
Middle Frontal Gyrus	L	2.4	−48, 12, 48
	R	2.7	45, 0, 42
Superior Temporal Gyrus	L	2.2	−48, 15, −27
	R	2.4	30, 9, −36
Culmen	L	2.3	−30, −51, −24
Extra-Nuclear	L	2.2	−3, 27, 12
	R	2.1	3, 24, 18
Supramarginal Gyrus	L	2.1	−51, −48, 33
Sub-Gyral	L	2.1	−33, −60, −9
Thalamus	R	2.1	9, −15, 15
Precentral Gyrus	L	2.0	−54, −3, 42

Region	Hemisphere	*Max T*	MNI coordinates x,y,z
Factor 2 association with spatial maps of executive control network - negative effects			
Middle Frontal Gyrus	L	2.1	−48, 12, 48
	R	2.8	45, 0, 42
Culmen	L	2.6	−36, −51, −24
Superior Temporal Gyrus	L	2.2	−45, 18, −30
	R	2.4	39, 21, −30
Thalamus	L	2.0	−12, −15, 9
	R	2.2	12, −15, 6
Precentral Gyrus	R	2.2	48, 0, 39
Extra-Nuclear	R	2.1	24, −15, 9
Sub-Gyral	L	2.0	−36, −3, 21
Insula	L	2.0	−39, −9, 0
Declive	L	2.0	−36, −54, −21
Factor 2 association with spatial maps of executive control network - positive effects			
Inferior Temporal Gyrus	L	2.9	−51, −21, −27
Inferior Frontal Gyrus	R	2.4	30, 21, −21
Cuneus	L	2.2	−9, −93, 24
Fusiform Gyrus	L	2.2	−51, −18, −30
Declive	L	2.1	−9, −81, −21
Parahippocampal Gyrus	L	2.0	−24, −18, −27

Note. Table shows all clusters with a maximum associations of $T > 2.0$